Drozdenko, D.; Bohlen, J.; Horvath, K.; Yi, S.; Letzig, D.; Chmelik, F.; Dobron, P.:

**Effect of Thermomechanical Treatment on Subsequent Deformation Behavior in a Binary Z1 Magnesium Alloy Studied by the Acoustic Emission Technique.**

In: Advanced Engineering Materials. Vol. 21 (2019) 3, 1800915.

First published online by Wiley: 27.12.2018

https://dx.doi.org/10.1002/adem.201800915

**Effect of Thermomechanical Treatment on Subsequent Deformation Behavior in a Binary Z1 Magnesium Alloy Studied by the Acoustic Emission Technique**

By *Daria Drozdenko**, *Jan Bohlen*, *Klaudia Horváth*, *Sangbong Yi*, *Dietmar Letzig*, *František Chmelík*, *Patrik Dobroň*

[*] *Dr. Daria Drozdenko Corresponding author*

1. *Department of Physics of Materials, Faculty of Mathematics and Physics, Charles University, Ke Karlovu 5, Prague 2, 12116, Czech Republic*
2. *Magnesium Research Center, Kumamoto University, 2 -39-1 Kurokami, Kumamoto, 860-8555, Japan*

*E-mail: drozdenko@karlov.mff.cuni.cz*

*Dr. Jan Bohlen, Dr. Sangbong Yi, Dr. Dietmar Letzig*

*Magnesium Innovation Centre, Helmholtz-Zentrum Geesthacht*

*Max-Planck-Straße 1, D21502 Geesthacht, Germany*

*Ms. Klaudia Horváth,*

1. *Department of Physics of Materials, Faculty of Mathematics and Physics, Charles University, Ke Karlovu 5, Prague 2, 12116, Czech Republic*
2. *Nuclear Physics Institute, The Czech Academy of Sciences Řež 130, 250 68, Řež, Czech Republic*

*Dr. František Chmelík, Dr. Patrik Dobroň*

*Department of Physics of Materials, Faculty of Mathematics and Physics, Charles University, Ke Karlovu 5, Prague 2, 12116, Czech Republic*

**Abstract**

Pre-straining of magnesium alloy modifies the final texture of the material and therefore leads to a different deformation behavior during subsequent loading. At the same time, heat treatment in the context of thermo-mechanical procedures can be used as softening mechanism, as well as for age hardening processing. In mechanical conditions with twin-dominated deformation in textured magnesium alloys, the twin boundaries can be pinned if existing after a pre-deformation of samples and therefore influence their mobility. The impact of the ongoing mechanical behavior has been discussed. In the present paper, a procedure of pre-compression and reverse tensile loading of extruded binary magnesium alloy Mg-1wt.% Zn (Z1) is used and intermediate aging at 200°C has been applied in two different routes. The effect of the heat treatment on the flow behavior during subsequent mechanical loading has been correlated with the dominating deformation mechanisms revealed by *in-situ* acoustic emission measurements and *ex-situ* scanning electron microscopy. The pinning of twin boundaries can restrict their mobility in experimental environments that favor the recovery of the samples. As a result, new twins easily nucleate if the concurrent re-orientation of the lattice is favorable for strain accommodation.

## 1. Introduction

The formation of a strong basal texture is a well-known phenomenon for wrought magnesium alloys. Such a characteristic texture together with the directionality of the twinning mechanism in the *hcp* lattice is responsible for their anisotropic mechanical properties. For enhancing mechanical properties of Mg alloys, besides variations in alloying composition, thermomechanical treatment has a potential to be exploited. In particular, the effect of either sole heat treatment (HT),[1-4] pre-straining,[5-8] or their proper combination [9-12] on mechanical properties of wrought Mg alloys has attracted interest during last decades.

In extruded Mg alloys, pre-compression along the extrusion direction (ED), i.e. perpendicular to the c-axis of the *hcp* lattice structure, introduces {10-12}<10-11> extension twins into the

microstructure.[13,14] Depending on the level of the pre-strain, various twin volume fractions can be achieved.[5,11] A resulting new texture component allows the activation of deformation mechanisms (dislocation slip and twinning), which are not promoted in the initial state before pre-straining. Therefore, pre-straining and a corresponding moderation of the deformation behavior during further loading can be used to reduce the tension-compression asymmetry of the mechanical properties.[7,8] During reverse loading of pre-compressed Mg alloys, detwinning – i.e. thickness reduction or complete disappearance of existing twin lamellae − becomes a key deformation mechanism.[8,15,16] Detwinning can be realized either by migration of already existing twin boundaries [17] or by secondary twinning inside existing twins.[9,18,19] *Ex-situ* and *in-situ* methods, such as electron backscattered diffraction (EBSD), high-speed imaging and acoustic emission (AE) technique, have been successfully used for investigations of the twinning-detwinning process during cyclic loading in Mg alloys.[18,20,21]

During a heat treatment, besides recovery processes, pinning of twin boundaries can take place. Nie at al.[22] have reported periodic segregation of Zn and Gd solute atoms in fully coherent twin boundaries, providing a pinning effect for the twin boundaries, which leads to a strengthening of the alloy. The control of the twinning-detwinning process by annealing in pure Mg, AZ31 and AZ91 has been recently studied by Cui et al.[9,10]. The effect of Al and Zn as solute elements and respective Al and Zn containing precipitates on the migration of atoms to the twin boundaries during detwinning was studied in particular. They concluded that the formation of secondary twins inside primary twins during reverse loading can be ascribed to the low mobility of the incoherent twin boundaries due to the hindering effect of precipitates. It was shown by Drozdenko et al.[19] that isothermal aging at 200°C for 8 h does not completely disrupt the mobility of twin boundaries, and twin thickening or shrinkage can be observed. However, it was indicated that solute segregation due to heat treatment can lead to the appearance of secondary twinning inside existing twins as a special mode of the detwinning process.

Based on the above-mentioned information it can be concluded that pre-compression and pinning of grain/twin boundaries by solute atoms results in the different yielding behavior during subsequent mechanical loading. However, it is not completely clear by which mechanisms the subsequent deformation of such thermomechanically treated samples is controlled.

Acoustic emission (AE) is an *in-situ* technique, which is based on acquiring transient elastic waves as a result of sudden release of energy due to a local dynamic change within a material, such as collective dislocation movement or twin nucleation.[23] AE is a powerful method for revealing the active deformation mechanisms and their development during loading. The AE technique was successfully used to investigate various metallic materials,[23-28] especially with a *hcp* lattice,[21, 29-32] as it is highly sensitive to twin nucleation.

The aim of this study is to explore the effect of pre-compression and the concurrent activation of dislocation slip and twinning on the mechanical response during subsequent tensile loading. Especially, the effect of intermediate isothermal aging with respect to the pinning of twin boundaries as well as with respect to the recovery process is investigated. AE measurements allow tracking the active deformation mechanisms while scanning electron microscopy (backscattered electron (BSE) imaging and EBSD mapping) provides information about the interaction of twin boundaries with precipitates. The obtained evidence can be useful for the development of Mg alloys with enhanced properties.

## 2. Experimental procedure

The binary Z1 magnesium alloy (Mg + 1 wt.%Zn) was extruded at 300°C with the extrusion ratio of 1:30. The extruded material is characterized by a homogeneous, fully recrystallized microstructure with an average grain size of ~ 50µm, see **Figure 1**. Basal planes are aligned parallel to the extrusion direction.

Samples with a gauge length of 15 mm, a diameter of 8 mm, and screw heads on both ends were machined from the round extruded profile to be tested in ED. Deformation tests were performed

in a universal testing machine Instron 5882 at room temperature. Loading was performed with a constant strain rate of $10^{-3}$ $s^{-1}$.

To reveal the effect of pre-compression and concurrent activation of dislocation slip and twinning on the mechanical response during subsequent loading after an intermediate heat-treatment of the samples, the following two testing routes were chosen:

Route I: pre-compression up to 100 MPa (5.6% of nominal strain), isothermal aging at 200°C for 8 h and reverse tensile loading up to 75 MPa;

Route II: pre-compression up to 75 MPa (2.7% of nominal strain), isothermal aging at 200°C for 8 h, re-compression up to 100 MPa (i.e. additional 3% of nominal strain) and reverse tensile loading up to 75 MPa.

These experimental routes were repeated to receive samples for microstructure evaluation after the respective segments of the experiments.

For monitoring the AE response, a computer-controlled PCI-2 device (Physical Acoustic Corporation) with a piezoelectric transducer (PICO - PAC, operating frequency range 200-750 KHz) and a 2/4/6-preamplifier giving a gain of 60 dB was used during deformation testing. The sensor was attached to the sample surface using vacuum grease and a clamp. The raw AE signal provides information about the AE peak amplitude: sources of low and high amplitude AE signals can be distinguished. Besides the raw AE signal, AE count rate ($\Delta NC/\Delta t$), which is the count number per unit time (0.1 s) at a given threshold voltage level,[33] was used to determine changes in collective dislocation processes and twinning activity. Thus, both the raw AE signal and the AE count rate are used for the characterization of active deformation mechanisms. Previously, combination of those parameters was effectively used for study on activity of the dislocation slip and twinning during compression of Mg single crystals.[30]

Information about the microstructure and texture development was obtained by a scanning electron microscopy (SEM) Zeiss Auriga, using particularly backscattered diffraction techniques: BSE imaging and EBSD mapping. For SEM observations, the specimens were polished in the

longitudinal plane by diamond pastes with the particle size decreasing down to 0.25 μm and subsequently electropolished using the Struers AC-2-II electrolyte. The EBSD mapping was carried out with a step size of 0.4 μm.

Growth and shrinkage of twins during re-compression and reverse loading, respectively, were especially investigated with respect to a possible pinning effect of twin boundaries after aging.

## 3. Results

The result of the deformation experiment along route I is plotted in **Figure 2a** together with the *in-situ* measured AE signal. The same is shown in **Figure 2b** but concurrent with the AE count rate. The AE signal gives a direct impression of the signal amplitudes whereas the count rate refers directly to the frequency of AE signal crossing the threshold level during the respective time intervals regardless of their amplitudes. By a combination of both parameters/characteristics the type of AE signal - continuous or burst, can be determined. Therefore, the proposed way of representing the data allows direct comparison of the applied stress to the AE signal and the count rate, referring to the global appearance of sources, such as dislocation glide avalanches or twins during loading, in the entire volume of the sample.

Route I in Figure 2 was divided into three sections: first - pre-compression up to 100 MPa (C-I), second - intermediate isothermal aging for 8 h at 200°C, and third - reverse tensile loading up to 75 MPa (T-I). As twinning and detwinning are assumed to take a major role in the presented deformation experiment, reverse loading was applied only up to 75 MPa, i.e. a lower stress level than during pre-compression (100 MPa), in order to avoid complete detwinning and retaining the possibility to analyze remaining twin boundaries.

The deformation curve during pre-compression is characterized by a sigmoidal (S-) shape and a pronounced yield plateau, which has been often associated with the preferential activation of extension twins. The compressive yield stress (CYS) of the as-extruded condition of the material is 57±1 MPa. During the macroelastic part the AE signal (Figure 2a) is characterized by medium AE

amplitudes, which grow gradually until the yield stress (YS) is achieved. At the same time, the AE count rate increases up to a local maximum. These features can be assigned with the continuous type of AE, which is characteristic for a collective dislocation motion.

At the yield point, the AE signal shows high amplitudes, while the AE count rate drops after the local maximum. This can be assigned to a prevalence of burst type of AE signals having a low count rate. With increasing the applied load after the yield point, the amplitude of the AE signal and the AE count rate gradually decrease. Exceeding certain strain, the amplitude level of the AE signals saturates whereas the count rate continues to decrease despite some points of high count rate at higher strain. The decrease of the AE signal is associated with a decrease of collective dislocation glide (e.g. as a result of work hardening) and/or a reduction of twin nucleation activity as an excellent AE source producing burst type signals. The decrease of the count rate refers to the lower activity of detectable AE sources and can also be associated with the work hardening of the sample.

After intermediate aging of the sample, reverse tensile loading (T-I) reveals a pronounced yield point at 71±1 MPa which is higher compared to the pre-compression segment (C-I) but lower compared to the maximum applied compressive stress of 100 MPa. After the yield point, the deformation curve exhibits a similar S-shape as in the previous pre-compression segment (C-I). The AE signal (Figure 2a) and the AE count rate (Figure 2b) are also similar to that for C-I, however, the AE amplitudes are lower. We can therefore assume that a continuous increase of collective dislocation motion in the macroelastic part is followed by twin nucleation. It is worthwhile to repeat that twin boundary movement during twin growth or twin shrinkage does not produce detectable AE.[25,34] Therefore, the nucleation of new twins can be hypothesized as a source of the high amplitude signals in the reverse tension segment T-I at the yield point.

In summary, the pre-compression part of the experiment by the Route I is likely to activate twining as a distinct deformation mechanism, which is followed by a typical S-shaped work hardening associated with the growth or thickening of twins. Intermediate aging leads to softening of the

material to some extent. During reverse tensile loading the nucleation of new twins becomes again a distinct deformation mechanism.

The deformation curves along Route II are correlated to the AE signal in **Figure 3a** and to the AE count rate in **Figure 3b**. In this experiment, the intermediate aging is shifted to an earlier point and conducted after the pre-compression phase to 75 MPa (C-II). In order to study its effect on the ongoing compression behavior, subsequent re-compression up to 100 MPa (CC-II) was applied. This is then again followed by reverse tensile loading (T-II) without additional aging. The pre-compression segment (C-II) shows the same behavior as presented above along with Route I but is stopped at lower stress. During re-compression (CC-II) after aging, a pronounced elastic limit is observed at 65±1 MPa, which is lower compared to the previously applied maximum stress level. Both the AE signal and the AE count rate show strong similarities to the previous pre-compression segment (C-II), only with lower amplitudes of the AE signals. It is noteworthy that this behavior is different compared to the respective stress range measured in the pre-compression segment of Route I (C-I). The indication of further twin nucleation as revealed from the AE during the CC-II segment is a result of the intermediate aging and was not seen in the same stress range in the previous experiment along Route I.

In the following reverse tensile loading segment (T-II), there is no pronounced elastic limit but a continuous decrease of the slope leading into a region of plastic deformation. A gradual increase in both the AE amplitudes (Figure 3a) and the AE count rate (Figure 3b) was observed. However, a change in the AE response is observed simultaneously with a change in the hardening behavior. AE events with a low AE count rate start to appear, and the AE signals with high amplitude become rather rare. Nonetheless, few AE events with high amplitudes can be observed during the entire loading.

For the two routes, different levels of pre-compression, namely C-I (100 MPa) and C-II (75 MPa), were applied to obtain microstructures with different twin volume fractions (TVF), which were found to be 38% and 16% of the analyzed area, respectively (**Figure 4a,c**). During further re-compression CC-II (up to 100 MPa) of the sample subjected to pre-compression up to 75 MPa and

HT, a TVF of 31% was found, **Figure 4d**. This value is lower than that for the sample without intermediate aging – C-I, Figure 4a.

TVF during reverse tensile loading decreases due to detwinning. As a result of a reduction or full disappearance of twin lamellae after reverse loading up to 75 MPa, TVF of the samples in the route I and II were of 20% and 25% of the analyzed area, respectively (**Figure 4b, e**). The above-described change in TVF is also reflected in the texture development, **Figure 5**. The twinned fraction of the microstructure appears with increasing intensity at the (0001)-pole which starts to develop in Figure 5c and is fully developed after the full compression phase in Figures 5a or 5d. The C-I segment of route I, without intermediate aging, results in a stronger development of the pole. The pole intensity decreases again with subsequent reverse tension, Figures 5b and 5e.

In order to reveal more details of the twinning-detwinning process with respect to the possible occurrence of a pinning effect, a BSE imaging was performed in addition to the EBSD mapping. In **Figures 6-7,** segregation of solute atoms and precipitates along twin and grain boundaries as a result of isothermal aging in both routes, I and II, is presented. During re-compression (CC-II) in the route II, one can observe (i) nucleation of a new twin in the grain, while already existing twin is prevented from growing by pinning of twin boundaries (Figure 7a) and (ii) thickening of twins with pinned twin boundaries (Figure 7b). In the framework of detwinning process, migration of pinned twin boundaries takes place in route I and II, cf. Figure 7c. Moreover, nucleation of the new twin inside primary twin with pinned twin boundaries appears during reverse loading as a special case of detwinning along the route I (Figure 6).

## 4. Discussion

The continuous type of the AE signal recorded before YS during **pre-compression for both experimental routes** (Figures 2 and 3) can be assigned to collective dislocation motion through the easily activated basal slip, which is typical for Mg alloys.[30,36] A relatively low critical resolved shear stress (CRSS) for the basal slip by comparison to the other slip modes gives rise to its preferential

activation during loading.[36,37] Due to higher CRSS for prismatic and pyramidal slip, tensile twinning becomes an important additional deformation mechanism in Mg and its alloys and thus it is activated once basal slip occurred. The high amplitude AE signal and the S-shaped deformation curve are usually associated with the twinning activity.[23,30,36] It is important to note that twin nucleation produces high amplitude AE signals, while twin propagation does not, as was shown in earlier works.[25,30,34] This fact was explained by a difference in the speed of twin nucleation and propagation in Mg and its alloys. Recently, the evidence of this phenomenon was shown by Vinogradov et al.[38] using synchronized AE measurements and rapid video imaging. Hence, the observed decrease of the AE parameters during further loading can be related to twin growth and, at the same time, to a decrease in the free path of moving dislocations. AE events with high AE amplitudes, appearing during the entire test, can be associated with the nucleation of new twins.

The twinning activity is reflected in the arising new texture component around the (0001) pole in Figure 5a,c and in highlighted twins in the orientation maps in Figure 4a,c. A different level of pre-compression leads to different TVF, which is 16% and 38% of the analyzed area for pre-compressions up to 75 MPa and 100 MPa, respectively. Moreover, in the case of higher pre-compression, twins succeed to reach grain boundaries and then propagate mostly perpendicularly to the twin plane (twin thickening). Resulting interaction area of the twin and grain boundaries is larger comparing to the area in the route II, where twins are mostly embedded inside the grains. Similarly, Cui et al.[9] reported two morphology groups of twins in the grain: narrow twins totally embedded inside the grain and large twins with their front tip merged with the grain boundary.

However, unloading up to the 0 MPa for performing isothermal aging in the route II (i.e. resulting relaxation processes) and HT itself (i.e. reduction of twins and dislocation recovery) also affect formation of final TVF. Therefore, a difference in TVF in the present study should be discussed with respect to those processes. A detailed analysis of this issue is beyond the scope of the present paper.

The sigmoidal shape of the deformation curve for the **reverse tensile loading** can be explained by the polar nature of twinning. Detwinning as a key mechanism was widely observed in Mg and its alloys, which were subjected to reverse loading.[8,16,20] In case of no heat treatment after the compression segment the detwinning is more favorable than twinning.[20] For example, results of Cui et al. indicated that detwinning proceeds in a much easier way than twin growth due to the presence of back stress after twinning.[9] In case of reverse loading **in route I**, besides twin shrinkage, detwinning is also realized by ~~a~~ nucleation of new twins in primary twins, which contain segregated atoms or precipitates at ~~the~~ twin boundaries, see Figure 6. The nucleation of new twins corresponds to high amplitude AE signals observed around YS, see Figure 2a. Detwinning *via* nucleation of secondary twins in a primary twin during reverse loading has been recently explained by a low mobility of twin boundaries.[9] Moreover, it was more significant for Mg alloys by comparison to pure Mg. Using misorientation analysis it was revealed that the orientation of the secondary twins is identical to the initial orientation of the lattice. This mode of detwinning was observed previously.[18,19] As a result of twin boundary migration, low angle boundaries were observed at the positions of the original twin boundaries after detwinning.[9,19] It can be concluded that detwinning is realized by the same twinning mode as twinning during the pre-straining.[16,39]

In the case of **re-compression in route II,** reactivation of twinning (i.e. propagation of already existing twins as well as nucleation of new ones) leads to the S-shaped curve. The decrease in YS value for re-compression from the stress level of the pre-strain can be explained by solute softening occurring in large grains (above 50 μm), where the minimum stress is required to cross slip.[35] Moreover, it was reported that the presence of solute reduces stress required for dislocation to cross slip into the prismatic plane and thus solute softening (of prismatic slip) can be observed.

Recovery processes due to HT after pre-compression in route II reduce the number of dislocations, which results in a "refreshed" microstructure. Therefore, in contrast to Kaiser effect,[40] when AE renews in material only after reaching the previous level of a load during repetitive loading, the significant AE response from a collective dislocation movement is observed even before YS, see

Figure 3. Pinning of twin boundaries reduces their mobility and sometimes can even completely prevent twins from growing. Therefore, nucleation of new twins takes place in a grain containing a prexisting twin with pinned boundaries. Robson et al. [41] showed that large precipitates can completely hinder twin growth, and twinning usually continues by nucleation of a new twin in the grain on the far side of the particle, while small particles can either become engulfed by a growing twin without shearing or they can be shared inside the twins.[42] Newly created twin boundaries free of precipitates can be seen in Figure 7a. Most of the grains continue to show nucleation of twins by the same variant of extension twins, which was active during pre-straining. This can be explained by a higher value of the Schmid factor for this variant of twin.[19] The high amplitude AE signal, observed at YS, Figure 3a, confirms a relatively high activity of new twin nucleation. However, some twins continue to grow, see Figure 7b. As twin growth and shrinkage itself in non-heat treated samples does not produce detectable AE, it is therefore suggested that *de-pinning of segregated twin boundaries* from their position results in a huge release of energy, i.e. high amplitude AE signals. In other words, after intermediate heat treatment high amplitude AE signals around YS originated from (i) new twin nucleation and (ii) de-pinning of segregated twin boundaries in the frame of twin growth or shrinkage. The result of twinning activity can be also seen in increasing values of TVF in Figure 4c-d and the intensity of twin texture component at the (0001) pole in Figure 5c-d. An additional strain of 3% results in twice larger TVF. The difference in TVF of the pre-strained samples up to the same level via route I and II (i.e. with applied HT in a different sequence), Figure 4b, d, can be explained by the suppression of the twinning activity due to unloading for performing HT in route II as well as HT itself in both routes. However, as mentioned above, other mechanisms, such as recovery, should be considered.

During **reverse loading in route II,** deformation is realized by detwinning and dislocation slip, which was not preferred during pre-straining due to the texture of the material. A diffuse or continuous activation of twin boundary migration together with the nucleation of new twins lead to a continuous decrease of the slope of the curve. Therefore, a pronounced yield point is missing in this case. Dislocation activity in “fresh” microstructure after detwinning is consistent with the gradual

intensification of the AE response, see Figure 3. Regarding detwinning, this process is mainly realized by twin boundary migration, Figure 7c. However, a nucleation of the new twin inside a primary twin with pinned twin boundaries – similarly to detwinning during T-I – is possible, as well. Most of the twins in the microstructures after thermomechanical treatment along the route I, i.e. before T-I, are characterized by a solute segregation along twin boundaries. In contrast, samples before reverse loading T-II are characterized by a microstructure with pinned twin boundaries as well as by "free twin boundaries" as a result of additional re-compression after HT. Therefore, a higher amount of mobile twin boundaries leads to detwinning, realized by the migration of existing twin boundaries (Figure 7c), not producing high amplitude AE. Figure 7c represents results of detwinning via migration of twin boundaries. At the prior twin boundary positions there is no segregation. It is therefore suggested that this twin was nucleated and grown during re-compression, CC-II. Subsequent reverse loading without intermediate HT between those two deformation parts is accompanied by easy migration of twin boundaries (marked by arrows in Figure 7c) without producing high amplitude AE. Increasing amplitudes before yielding during T-II, can be assigned to basal dislocation slip. The release of energy due to de-pinning of twin boundaries from the segregations (during detwinning) as well as possible nucleation of the new twin can lead to a high amplitude AE signal, what was rarely observed during T-II. However, saturation of the AE count rate after yielding and relatively low amplitudes of AE during entire reverse loading T-II are characteristics of a continuous type of the AE signal. It can be therefore concluded that recorded AE during reverse tensile loading in route II is rather result of a dislocation activity. Microstructure and texture development (Figures 4-5) also represent ~~the~~ results of detwinning: TVF as well as the intensity of the twin texture component around the (0001) pole decrease. The reasons for a 5% difference in TVF are seen in the variety in active deformation mechanisms prevailing during detwinning as well as relaxation, reduction of twins by HT, recovery of dislocations.

## 4. Conclusions

The effect of pre-compression and concurrent activation of slip and twinning as well as intermediate isothermal aging on the mechanical response during subsequent tensile loading has been studied by acoustic emission technique.

During pre-compression the basal slip is active, resulting in low-amplitude AE signal before yielding. High-amplitude AE signals appear around the yield plateau of the deformation curve, which is attributed to a massive twin nucleation. Interactions of gliding dislocations result in work hardening, which can be changed by intermediate aging, promoting recovery mechanisms. Furthermore, the heat treatment can lead to solute pinning effects of existing twin boundaries. A part of the twin boundaries is arrested by solute atoms and/or precipitates, preventing their propagation, and the nucleation of new twins becomes more favorable. During reverse loading after aging (route I) detwinning is forced to proceed by (1) migration of pinned twin boundary and by (2) activation of new twins inside existing twin lamellae, indicated by a burst type of AE signal. A continuous type of AE signal recorded before yielding is related to basal dislocation slip. If no aging is carried out before reverse tensile loading (route II), the observed continuous type of the AE signal with increasing amplitudes is assigned to higher dislocation activity, presumably basal slip. The reduction of the twinned volume fraction, in this case, proceeds by the migration of existing twin boundaries. Although recovery leads to a softening of the material during intermediate aging and to a reduction of the resulting YS; twin boundary pinning leads to a reduction of the twin boundary mobility. As a result, the nucleation of new twins proceeds, representing a prominent deformation mechanism.

## Acknowledgments

*This work received support from the Czech Science Foundation under grant 17-21855S (PD, FC, DD, KH, JB, SY, DL); the Operational Programme Research, Development and Education, The Ministry of Education, Youth and Sports (OP RDE, MEYS) under the grant CZ.02.1.01/0.0/0.0/16_013/0001794. KH is also grateful to the grant SVV-2018-260342. JB, SY, DL*

*also appreciate funding by the Deutsche Forschungsgemeinschaft (grant number BO 2461/4-1; YI 103/2-1).*

**Conflict of Interest.** The authors declare no conflict of interest.

**References:**

[1] J.F. Nie, B.C. Muddle, *Scr. Mater.* **1997**, *37(10)*, 1475.

[2] M. Bian, Z. Zeng, S. Xu, W. Tang, C.H.J. Davies, N. Birbilis, J.-f. Nie, *Metall. Mater. Trans. A*, **2016**, *47(12)*, 5709.

[3] J. Jain, P. Cizek, W.J. Poole, M.R. Barnett, *Mater. Sci. Eng., A*, **2015**, *647*, 66.

[4] P. Hidalgo-Manrique, J.D. Robson, M.T. Pérez-Prado, *Acta Mater.*, **2017**, *124*, 456.

[5] J. Bohlen, P. Dobron, L. Nascimento, K. Parfenenko, F. Chmelik, D. Letzig, *Acta Phys. Pol., A*, **2012**, *122(3)*, 444.

[6] Y. Jiang, Y.A. Chen, G.T. Gao, *Mater. Des.* **2016**, *97*, 131.

[7] J. He, T. Liu, S. Xu, Y. Zhang, *Sci. Eng., A*, **2013**, *579*, 1.

[8] Y.N. Wang, J.C. Huang, *Acta Mater.*, **2007**, *55(3)*, 897.

[9] Y. Cui, Y. Li, Z. Wang, X. Ding, Y. Koizumi, H. Bian, L. Lin, A. Chiba, *Int. J. Plast.*, **2017**, *91*, 134.

[10] Y. Cui, Y. Li, Z. Wang, Q. Lei, Y. Koizumi, A. Chiba, *Int. J. Plast.*, **2017**, *99*, 1.

[11] S.H. Park, J.H. Lee, Y.-H. Huh, S.-G. Hong, *Scr. Mater.* **2013**, *69(11)*, 797.

[12] Z. Long, T. Liu, Y. Wu, Y. Zhang, *Mater. Sci. Eng., A*, **2014**, *616*, 240.

[13] R.E. Reed-Hill, Inhomogeneity of Plastic Deformation, Metals Park, OH, **1973**.

[14] M.R. Barnett, *Mater. Sci. Eng., A*, **2007**, *464(1-2)*, 1.

[15] X.Y. Lou, M. Li, R.K. Boger, S.R. Agnew, R.H. Wagoner, *Int. J. Plast.*, **2007**, *23(1)*, 44.

[16] A. Chapuis, Y.C. Xin, X.J. Zhou, Q. Liu, *Mater. Sci. Eng., A*, **2014**, *612*, 431.

[17] M.A. Gharghouri, G.C. Weatherly, J.D. Embury, J. Root, *Philos. Mag. A*, **1999**, *79(7)*, 1671.

[18] K.D. Molodov, T. Al-Samman, D.A. Molodov, *Acta Mater.*, **2017**, *124*, 397.

[19] D. Drozdenko, P. Dobroň, S. Yi, K. Horváth, D. Letzig, J. Bohlen, *Mater. Charact.*, **2018**, *139*, 81.

[20] D. Drozdenko, J. Bohlen, S. Yi, P. Minárik, F. Chmelík, P. Dobroň, *Acta Mater.*, **2016**, *110*, 103.

[21] A. Vinogradov, E. Vasilev, M. Linderov, D. Merson, *Mater. Sci. Eng., A*, **2016**, *676*, 351.

[22] J.F. Nie, Y.M. Zhu, J.Z. Liu, X.Y. Fang, *Science*, **2013**, *340(6135)*, 957.

[23] C.R. Heiple, S.H. Carpenter, *J. Acoust. Emiss.*, **1987**, *6(3)*, 177.

[24] R.M. Fisher, J.S. Lally, Microplasticity detected by an acoustic technique, *Can. J. Phys.*, **1967**, *45(2)*, 1147.

[25] J.P. Toronchuk, *Mater. Eval.*, **1977**, *35(10)*, 51.

[26] I.V. Shashkov, T.A. Lebedkina, M.A. Lebyodkin, P. Dobron, F. Chmelik, R. Kral, K. Parfenenko, K. Mathis, *Acta Phys. Pol., A*, **2012**, *122(3)*, 430.

[27] F. Chmelík, E. Pink, J. Król, J. Balík, J. Pešička, P. Lukáč, *Acta Mater.*, **1998**, *46(12)*, 4435.

[28] A. Vinogradov, V. Patlan, S. Hashimoto, *Philos. Mag. A*, **2001**, *91(6)*, 1427.

[29] J. Balik, P. Dobron, F. Chmelik, R. Kuzel, D. Drozdenko, J. Bohlen, D. Letzig, P. Lukac, *Int. J. Plast.*, **2016**, *76*, 166.

[30] D. Drozdenko, J. Bohlen, F. Chmelik, P. Lukac, P. Dobron, *Mater. Sci. Eng., A*, **2016**, *650*, 20.

[31] K. Mathis, G. Csiszar, J. Capek, J. Gubicza, B. Clausen, P. Lukas, A. Vinogradov, S.R. Agnew, *Int. J. Plast.*, **2015**, *72*, 127.

[32] P. Dobroň, J. Balík, F. Chmelík, K. Illková, J. Bohlen, D. Letzig, P. Lukáč, *J. Alloys Compd.*, **2014**, *588*, 628.

[33] Standard Practice for Acoustic Emission Examination of Fiberglass Reinforced Plastic Resin (FRP) Tanks/vessels **2011**.

[34] C.R. Heiple, S.H. Carpenter, *J. Acoust. Emiss.*, **1987**, *6(4)*, 215.

[35] N. Stanford, M.R. Barnett, *Int. J. Plast.*, **2013**, *47*, 165.

[36] E.W. Kelley, W.F. Hosford, *Trans. Metall. Soc. AIME*, **1968**, *242(1)*, 5.

[37] B.C. Wonsiewicz, W.A. Backofen, *Trans. Metall. Soc. AIME*, **1967**, *239(9)*, 1422.

[38] A. Vinogradov, E. Vasilev, M. Seleznev, K. Máthis, D. Orlov, D. Merson, *Mater. Lett.*, **2016**, *183*, 417.

[39] J. Capek, K. Mathis, B. Clausen, J. Straska, P. Beran, P. Lukas, *Mater. Sci. Eng., A*, **2014**, *602*, 25.

[40] J. Kaiser, TU München, Germany **1950**.

[41] J.D. Robson, N. Stanford, M.R. Barnett, *Metall. Mater. Trans. A*, **2013**, *44a(7)*, 2984.

[42] M.A. Gharghouri, G.C. Weatherly, J.D. Embury, *Philos. Mag. A*, **1998**, *78(5)*, 1137.

**List of figure captions:**

Figure 1. Microstructure and texture of the extruded Z1 alloy in the initial state.

Figure 2 AE response: (a) raw AE signal, (b) count rate and stress vs. time dependences for deformation experiment along route I (pre-compression up to 100 MPa and after intermediate heat treatment reverse tension up to 75 MPa). For labels of segments of the experiment (C-I, T-I) the reader is referred to the text.

Figure 3 AE response: (a) raw AE signal, (b) count rate and stress vs. time dependences for deformation experiment along route II (pre-compression up to 75 MPa, after intermediate heat treatment re-compression up to 100 MPa and following reverse tensile loading up to 75 MPa). For labels of segments of the experiment (C-II, CC-II, T-II) the reader is referred to the text.

Figure 4 Microstructure and twin volume fraction of Z1 magnesium alloy after:

- route I: (a) pre-compression up to 100 MPa and (b) intermediate heat treatment and reverse tension up to 75 MPa;
- route II: (c) pre-compression up to 75 MPa, (d) intermediate heat treatment and re-compression up to 100 MPa followed by (e) reverse tensile loading up to 75 MPa.

Figure 5 Inverse pole figures of Z1 magnesium alloy after:

- route I: (a) pre-compression up to 100 MPa and (b) intermediate heat treatment and reverse tension up to 75 MPa;
- route II: (c) pre-compression up to 75 MPa, (d) intermediate heat treatment and re-compression up to 100 MPa followed by (e) reverse tensile loading up to 75 MPa.

Figure 6 BSE images of Z1 Mg alloy after the route I: pre-compression up to 100 MPa, intermediate heat treatment and reverse tension up to 75 MPa.

Figure 7 BSE images of Z1 Mg alloy after the route II: pre-compression up to 75 MPa, intermediate isothermal aging at 200°C for 8 h and re-compression up to 100 MPa (a-b) and reverse tensile loading up to 75 MPa (c).

**Figures:**

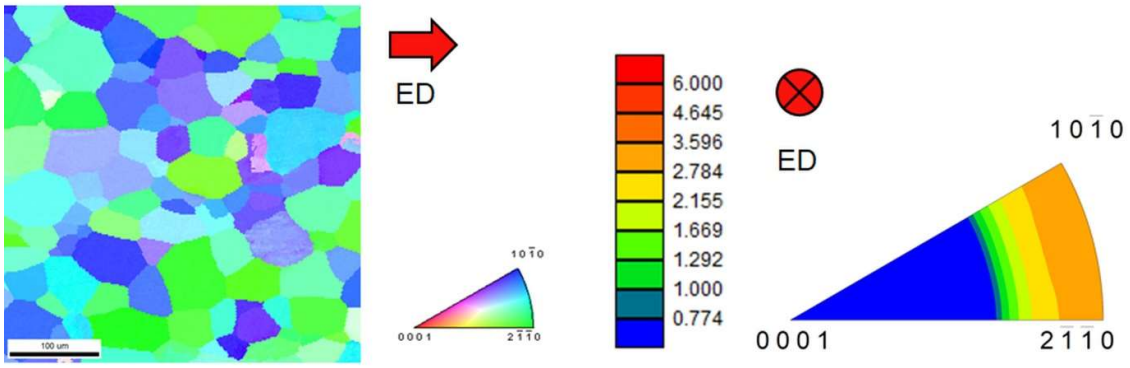


**Figure 1**

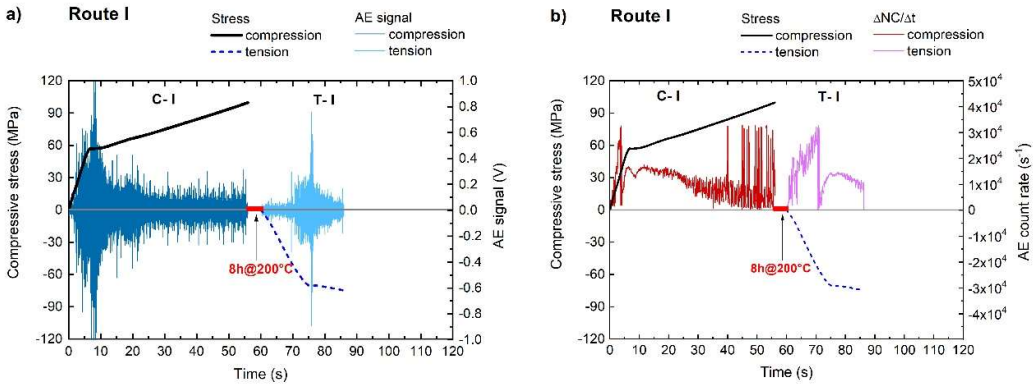


**Figure 2**

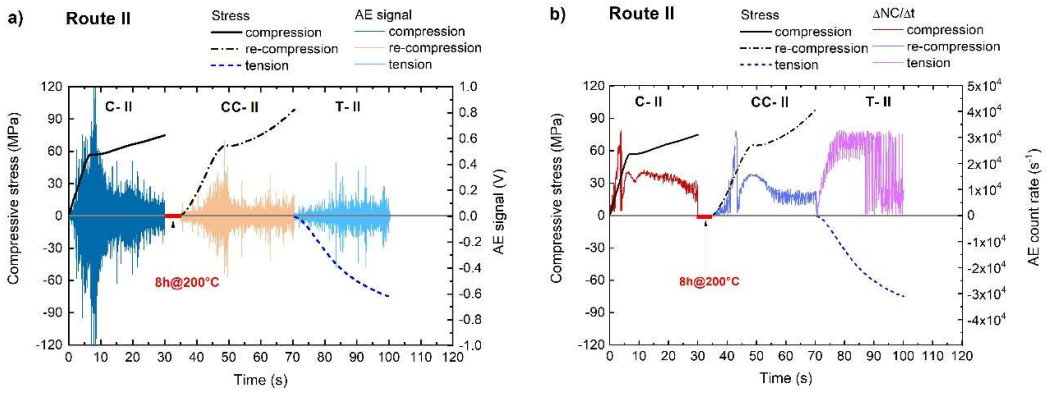


**Figure 3**

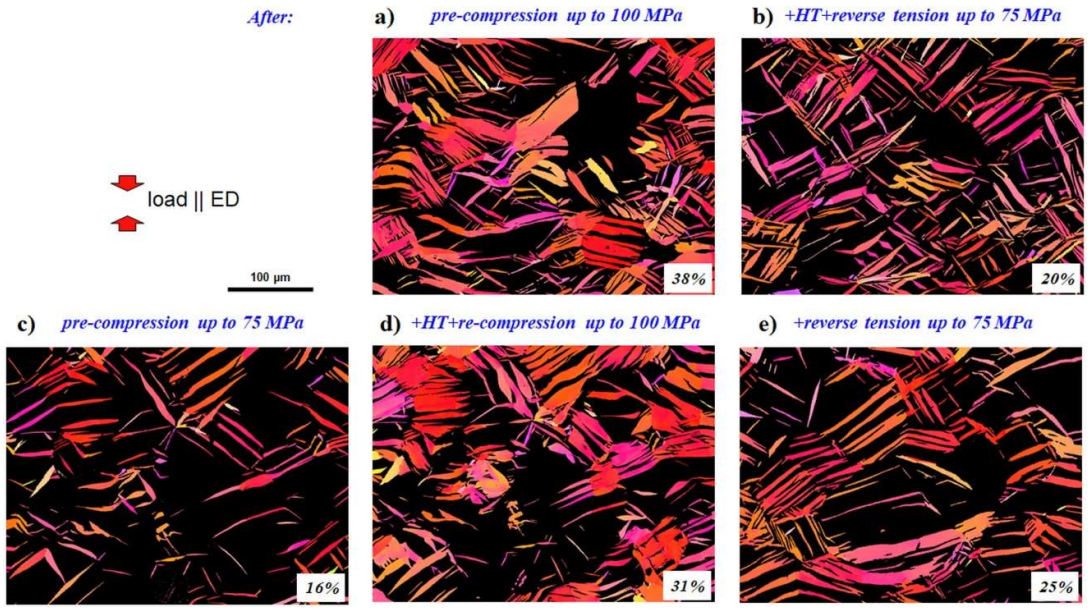


**Figure 4**

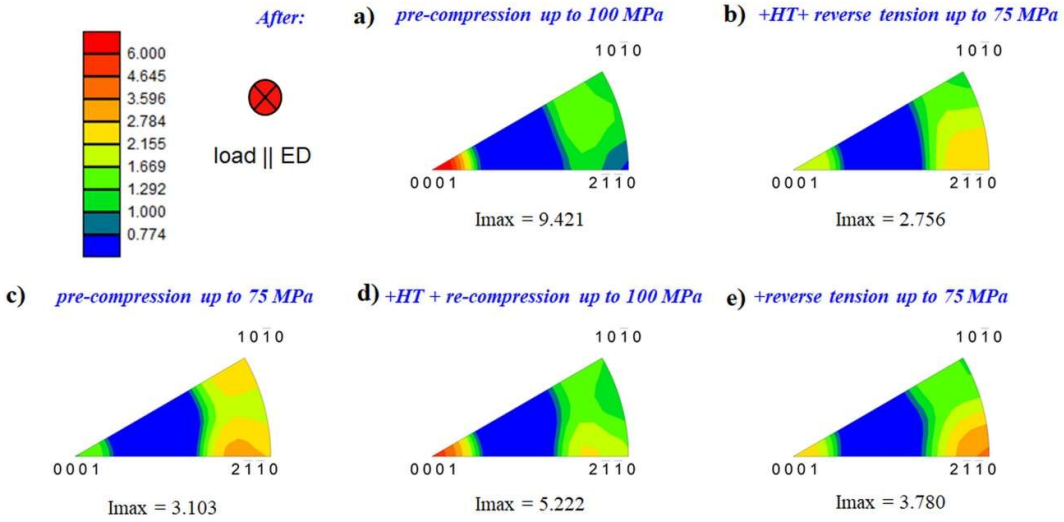


**Figure 5**

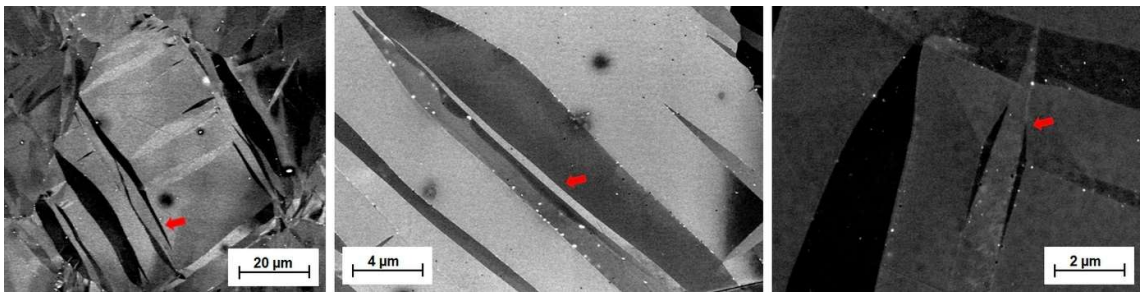


**Figure 6**

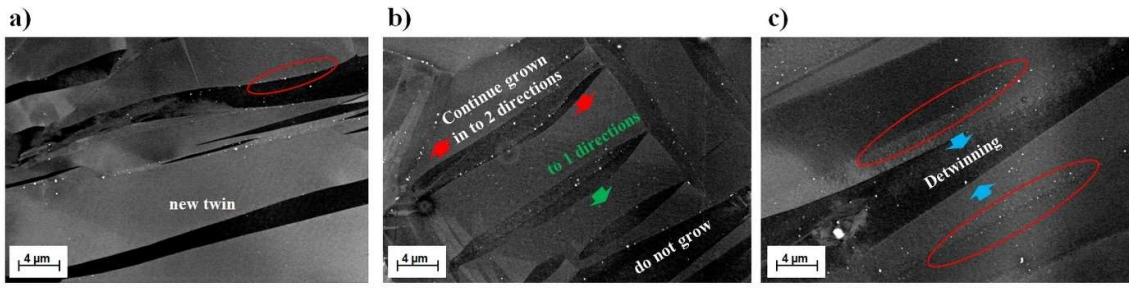
a)
b)
c)
new twin
4 μm
Continue grown in to 2 directions
to 1 directions
do not grow
4 μm
Detwinning
4 μm

**Figure 7**

**Table of Contents:**

By *Daria Drozdenko**, *Jan Bohlen*, *Klaudia Horváth*, *Sangbong Yi*, *Dietmar Letzig*, *František Chmelík*, *Patrik Dobroň*

**Title:**
**Effect of Thermomechanical Treatment on Subsequent Deformation Behavior in a Binary Z1 Magnesium Alloy Studied by the Acoustic Emission Technique**

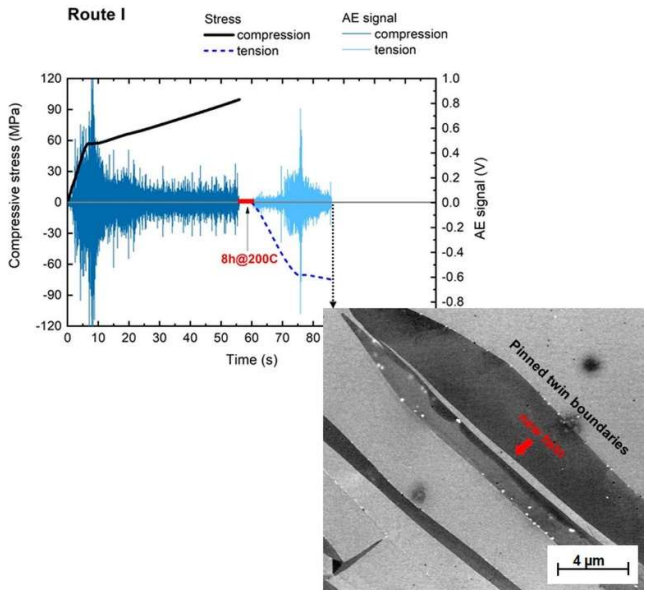


The effect of pre-compression and concurrent activation of slip and twinning as well as intermediate isothermal aging on the mechanical response during subsequent tensile loading has been elucidated by acoustic emission technique. Detwinning can proceed by migration of pinned twin boundary and by activation of new twins inside existing twin lamellae.